

ARM Science Team Meeting 2007

Comparison of aerosol optical depth from passive and active measurements during the 2005 Aerosol Lidar Validation Experiment (ALIVE) at SGP

Peter Kiedron¹, Connor Flynn², Richard Ferrare³, Brent Holben⁴, Joseph Michalsky⁵, Beat Schmid⁶ and James Slusser⁷

¹ CIRES/NOAA/Earth System Research Laboratory, peter.kiedron@noaa.gov

² Pacific Northwest National Laboratory, connor.flynn@pnl.gov

³ NASA Langley Research Center, richard.a.ferrare@nasa.gov

⁴ NASA/Goddard Space Flight Center, brent@spamer.gsfc.nasa.gov

⁵ NOAA/Earth System Research Laboratory, joseph.michalsky@noaa.gov

⁶ Pacific Northwest National Laboratory, beat.schmid@pnl.gov

⁷ Colorado State University, sluss@uvb.nrel.colostate.edu

ABSTRACT: During the Aerosol Lidar Validation Experiment (ALIVE) conducted from Sep 12 to 22, 2005 at the Department of Energy (DOE) Southern Great Plains (SGP) ARM Climate Research Facility (ACRF) in Oklahoma, the NASA Ames Airborne Tracking 14-channel Sun photometer (AATS-14) was flown aboard a profiling aircraft to measure aerosol extinction profiles. The chief goal of this experiment was to validate extinction profiles obtained with active measuring instruments: Raman Lidar (at 355nm) and Micro-Pulse Lidar (MPL at 523nm). Aerosol Optical Depth (AOD) was retrieved from the Raman Lidar through integration of vertical extinction profiles measured with the lidar. This integrated quantity was compared with column AOD retrieved from five independently calibrated passive radiometers and sun photometers: Two ARM and one USDA visible-wavelength (5 channels, 415 nm to 870 nm) Multi-Filter Rotating Shadowband Radiometer (MFRSR) from ARM, one USDA UV-MFRSR (6 channels, 305 nm to 368 nm), one Aeronet Cimel Sun Photometer (7 channels, 340 nm to 1020 nm), and one ARM Rotating Shadowband Spectroradiometer (999 pixels from 362 nm to 1070 nm). The AOD at 355nm from Raman Lidar was compared with interpolated values from AATS, UV-MFRSR and Cimel and the extrapolated values from RSS. All four Sun photometers correlate well at 355nm and AOD's agree within $\pm 0.03\text{OD}$. Raman Lidar results exhibit almost no bias ($< 0.006\text{OD}$) however they produce the largest standard deviation ($> 0.07\text{OD}$). For wavelengths longer than 380nm all five Sun photometers read within 0.01OD at all channels except for three channels of USDA's MFRSR at 415nm ($+0.02\text{OD}$), 610nm (-0.09OD) and 870nm ($+0.02\text{OD}$).

Aerosol Optical Depth Retrieval with Sun Photometers

$$\tau_a \approx \tau_a \cdot \frac{m_a}{m_R} = -\frac{1}{m_R} \ln \frac{I}{I_0} - \tau_R - \tau_{O_3} \cdot \frac{m_{O_3}}{m_R} - \tau_{O_2-O_2} \cdot \frac{m_{O_2-O_2}}{m_R} - \tau_{NO_2} \cdot \frac{m_{NO_2}}{m_R} - \tau_{H_2O} \cdot \frac{m_{H_2O}}{m_R}$$

Note: The assumption $m_a/m_R=1$ is always valid for small sun zenith angles. One may estimated that for $m_R=4, 6$ and 8 $m_a/m_R \approx 1.01, 1.03$ and 1.05 , respectively if aerosol profile is similar to water vapor profile. For very large air masses the knowledge of aerosol profile is essential for accurate retrieval of AOD.

TABLE 1. Sun photometers participating in ALIVE 2005⁸

| Sun Photometers | Instrument Characteristics | | | Applied Corrections and Calibration Method | | | | | | | |
|------------------------------------|-------------------------------------|----------------------|---------------|--|----------|----------------|--------------------------------|-----------------|------------------|------------------------------------|-----------------|
| | Channel ⁹ centroids [nm] | Resolution fwhm [nm] | Sampling rate | m_a | Rayleigh | O ₃ | O ₂ -O ₂ | NO ₂ | H ₂ O | Calibration for I/I ₀ | Cloud Screening |
| AATS (airborne) | 10: 353,...,1018 | 2.02 – 5.57 | | | yes | yes | | yes | | Langley on Mauna Loa ¹⁰ | |
| Cimel | 7: 340,...,1020 | 1.71 – 10.25 | ≈1/15min | | yes | yes | | | | Aeronet Procedure ¹¹ | yes |
| MFRSR _{C1&E13} | 5: 415,...,869 | ≈10 | 1/20sec | no | yes | yes | | no | | In situ Langley | yes |
| MFRSR _{USDA} | 5: 410,..., 860 | ≈10 | 1/3min | no | yes | | | | | In situ Langley | |
| UV-MFRSR _{USDA} | 2: 332 & 368 | 1.65 & 2.13 | 1/3min | no | yes | | n/n | n/n | n/n | In situ Langley | |
| RSS | 999: 362-1070 | 0.44 – 3.82 | 1/1min | no | yes | yes | yes | no | no | In situ Langley & Lamp 1/2weeks | no |

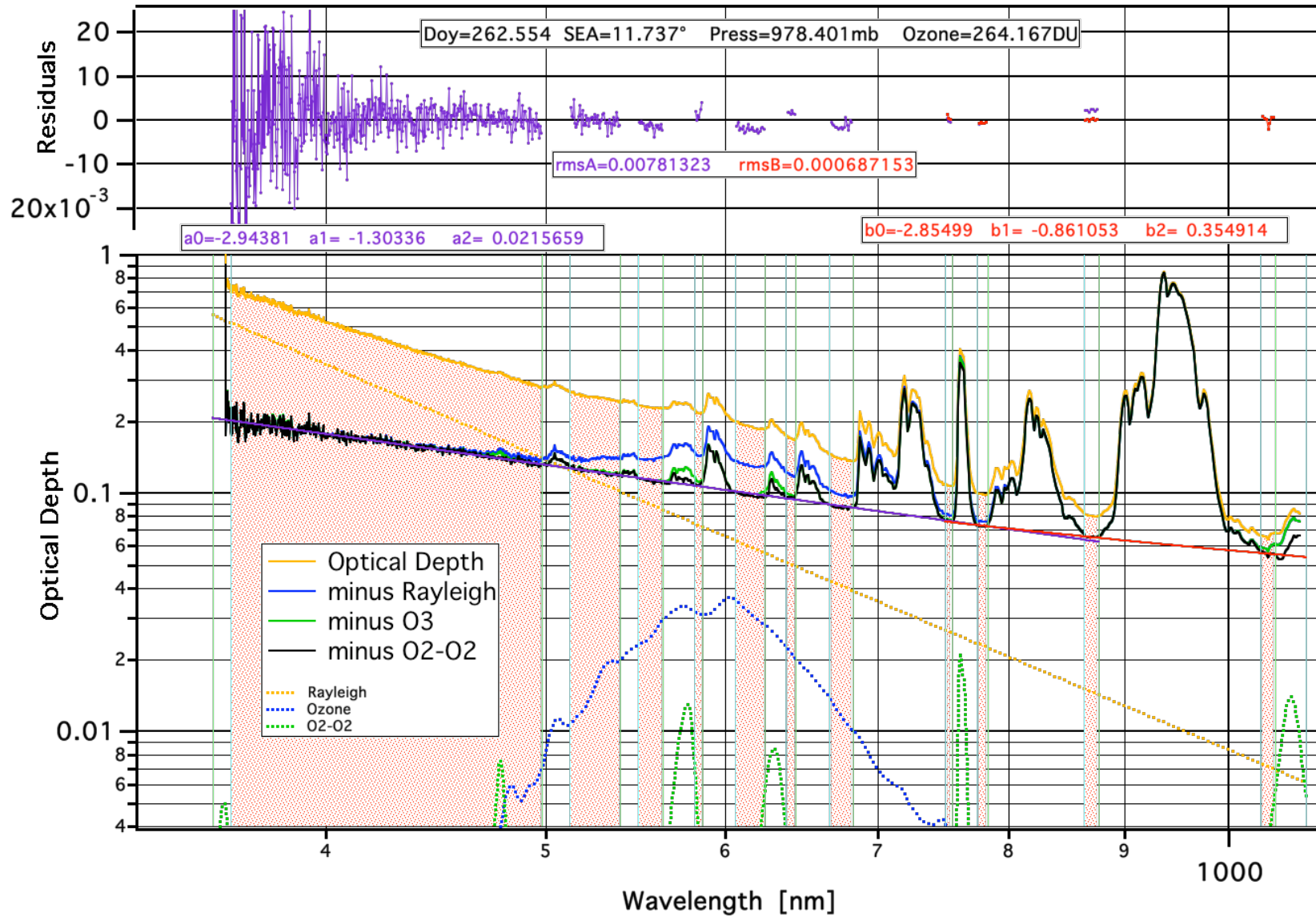
⁸ This table is incomplete. Missing information will be provided by co-authors. PK will appreciate references to formulas used (air mass, etc.) and to sources of x-sections (ozone, oxygen dimer, water, and nitrogen dioxide).

⁹ Only channels used in the comparison are indicated here. The near IR (>1070nm) channels of AATS had no counterparts in other instruments for comparison.

¹⁰ Langley calibration of AATS was performed before and after ALIVE campaign.

¹¹ The level 2 data are provided after transfer of calibration from collocated “master” Cimel. This necessitates Cimel de-fielding and results in intermissions between Cimel performances.

Example of AOD retrieval with RSS



Comparison methodology

RSS (1/min) data were cloud screened using MFRSR_{C1} cloud screened data set. Then for each instrument and channel a subset of data points was created that had RSS counterparts within 1 minute. The actual value of the centroid λ_k for a given channel was used to calculate $AOD_{RSS}(\lambda_k)$ from a trinomial Angstrom equation fitted to RSS AOD's. For wavelengths shorter than 362nm the same Angstrom equation was used to extrapolate AOD. So, RSS was used to compare with all channels including 332nm channel from UV-MFRSR, 340nm channel from Cimel, 353nm channel from AATS and 355nm channel from Raman Lidar.

From AATS, Cimel and UV-MFRSR bracketing wavelengths AOD at 355nm was logarithmically interpolated to use in comparison with Raman Lidar data.

In Tables 2 and 3 each subset used in comparison is characterized by its size N_{pnts} , airmass range A_{min} and A_{max} , start and end (d_{min} , d_{max}) times and by the range (y_{min} , y_{max}), mean μ_y and standard deviation σ_y of AOD values in the subset. The statistics from comparing $y=AOD(\lambda_k)$ and $x=AOD_{RSS}(\lambda_k)$ include: mean μ_{y-x} and standard deviation σ_{y-x} of differences, correlation $\rho_{(y,x)}$, slope α , intercept β and root mean square rms_{fit} of residuals from the linear fit $y=\alpha x+\beta$.

Two sets of AATS data were used: one contained AOD's as measured at a given altitude (90m-300m above ground) within 0.13km-9.8km from ACRF site and the other set had AOD's extrapolated to the ground level using the nearest available extinction profile from AATS flights.

Also Raman Lidar had two data sets (sampled 1/10min 24h/day) both at 355nm: one had AOD's from backscatter signal and the other from nitrogen N₂ signal.

In calculations, outliers are not removed and they are not treated differently.

Results of Comparison

TABLE 2. AOD from six instruments compared with RSS – cloud screening from MFRSR_{C1}

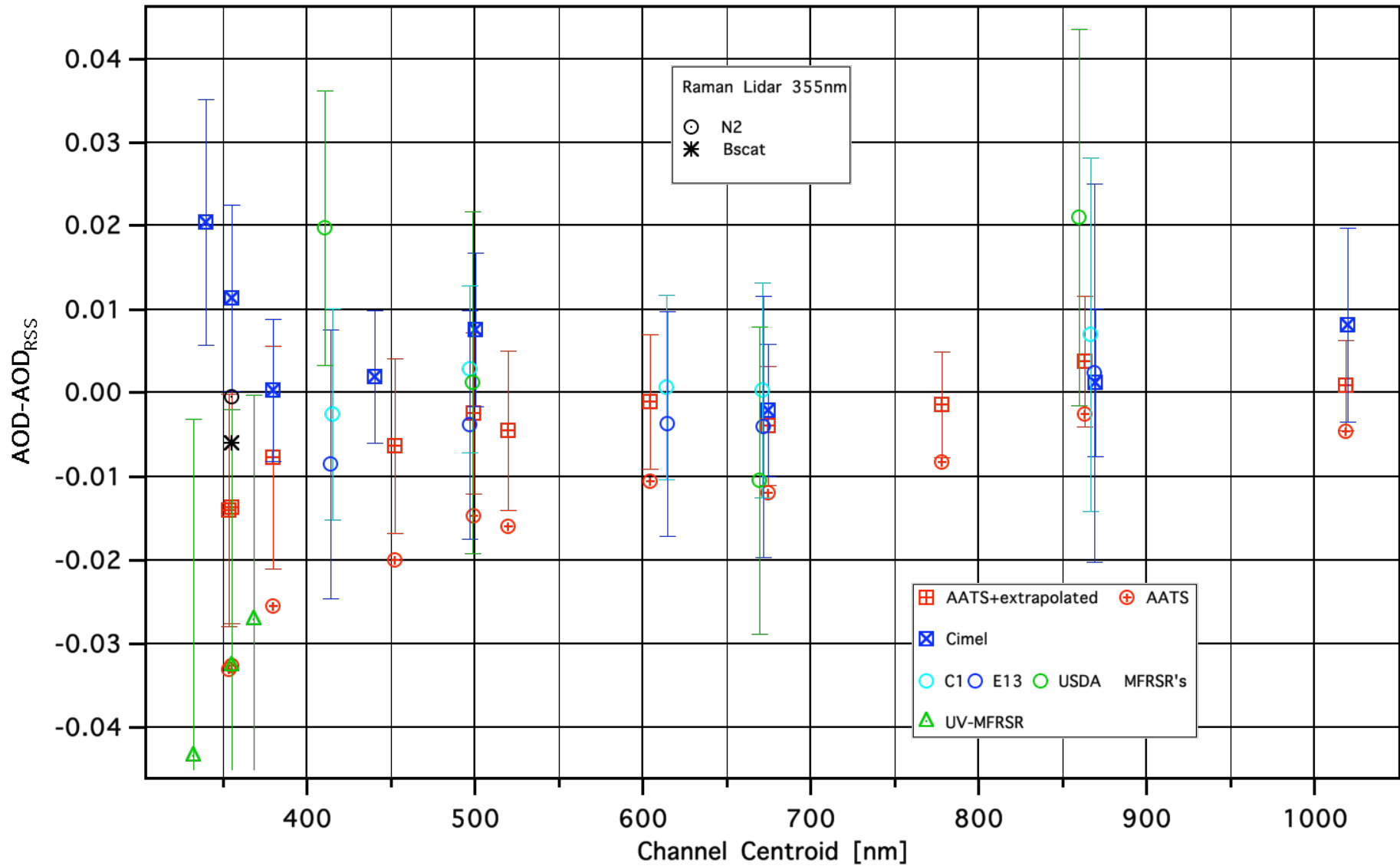
| Instrument | Channel centroids λ [nm] | Data Subset Characteristics | | | | | | | | Comparison with RSS | | | | | | |
|---------------------------|-------------------------------------|-----------------------------|------------------|------------------|------------------|------------------|------------------|---------|-------------|---------------------|---|----------------|----------------|----------|---------|--------------------|
| | | N_{pnts} | Airmass | | Time [doy] | | $y=\text{AOD}$ | | | | $y=\alpha x+\beta, x=\text{AOD}_{\text{RSS}}$ | | | | | |
| | | | A_{min} | A_{max} | d_{min} | d_{max} | y_{min} | μ_y | $2\sigma_y$ | y_{max} | μ_{y-x} | σ_{y-x} | $\rho_{(y,x)}$ | α | β | rms_{fit} |
| Cimel | 339.67 | 330 | 1.21 | 4.70 | 258.9 | 273.8 | 0.11 | 0.26 | 0.22 | 0.66 | 0.020 | 0.015 | 0.991 | 1.027 | 0.014 | 0.014 |
| | 355.00 ^{INTERP} | | | | | | 0.10 | 0.24 | 0.21 | 0.63 | 0.011 | 0.011 | 0.994 | 1.023 | 0.006 | 0.011 |
| | 379.89 | | | | | | 0.08 | 0.21 | 0.19 | 0.58 | 0.000 | 0.008 | 0.996 | 1.017 | -0.003 | 0.008 |
| | 440.15 | | | | | | 0.06 | 0.17 | 0.17 | 0.51 | 0.002 | 0.008 | 0.996 | 1.029 | -0.003 | 0.008 |
| | 500.35 | | | | | | 0.05 | 0.15 | 0.15 | 0.44 | 0.008 | 0.009 | 0.993 | 1.045 | 0.001 | 0.009 |
| | 674.71 | | | | | | 0.02 | 0.09 | 0.09 | 0.27 | -0.002 | 0.008 | 0.986 | 1.035 | -0.005 | 0.008 |
| | 869.67 | | | | | | 0.02 | 0.07 | 0.07 | 0.18 | 0.001 | 0.009 | 0.966 | 1.074 | -0.004 | 0.009 |
| | 1019.82 | | | | | | 0.02 | 0.06 | 0.06 | 0.15 | 0.008 | 0.012 | 0.929 | 1.143 | 0.000 | 0.011 |
| MFRSR _{C1} | 415.15 | 7614 | 1.14 | 5.99 | 244.5 | 273.8 | 0.07 | 0.31 | 0.34 | 0.86 | -0.003 | 0.013 | 0.997 | 1.006 | -0.005 | 0.013 |
| | 496.76 | | | | | | 0.06 | 0.23 | 0.25 | 0.67 | 0.003 | 0.010 | 0.997 | 1.021 | -0.002 | 0.010 |
| | 613.90 | | | | | | 0.04 | 0.16 | 0.17 | 0.47 | 0.001 | 0.011 | 0.991 | 1.013 | -0.002 | 0.011 |
| | 671.25 | | | | | | 0.04 | 0.14 | 0.14 | 0.40 | 0.000 | 0.013 | 0.982 | 0.987 | 0.002 | 0.013 |
| | 866.60 | | | | | | 0.03 | 0.09 | 0.08 | 0.24 | 0.007 | 0.021 | 0.868 | 0.781 | 0.026 | 0.019 |
| MFRSR _{E13} | 413.75 | 7349 | 1.14 | 5.99 | 244.5 | 273.8 | 0.06 | 0.30 | 0.34 | 0.81 | -0.009 | 0.016 | 0.995 | 1.011 | -0.012 | 0.016 |
| | 496.95 | | | | | | 0.05 | 0.23 | 0.25 | 0.63 | -0.004 | 0.014 | 0.994 | 1.026 | -0.010 | 0.013 |
| | 614.56 | | | | | | 0.03 | 0.16 | 0.17 | 0.45 | -0.004 | 0.013 | 0.987 | 1.019 | -0.007 | 0.013 |
| | 671.73 | | | | | | 0.03 | 0.13 | 0.14 | 0.39 | -0.004 | 0.016 | 0.974 | 0.989 | -0.003 | 0.016 |
| | 869.17 | | | | | | 0.02 | 0.09 | 0.08 | 0.24 | 0.002 | 0.023 | 0.842 | 0.774 | 0.022 | 0.021 |
| MFRSR _{USDA} | 410.39 | 911 | 1.25 | 3.83 | 265.6 | 273.8 | 0.10 | 0.24 | 0.23 | 0.70 | 0.020 | 0.016 | 0.990 | 1.004 | 0.019 | 0.016 |
| | 498.50 | 3525 | 1.14 | 3.88 | 244.6 | 273.8 | 0.05 | 0.23 | 0.26 | 0.86 | 0.001 | 0.020 | 0.988 | 1.044 | -0.009 | 0.020 |
| | 609.01 | | | | | | 0.00 | 0.08 | 0.10 | 0.74 | -0.093 | 0.041 | 0.912 | 0.553 | -0.014 | 0.020 |
| | 669.22 | | | | | | 0.02 | 0.13 | 0.13 | 0.78 | -0.011 | 0.018 | 0.964 | 0.916 | 0.001 | 0.017 |
| | 859.66 | | | | | | 0.03 | 0.11 | 0.09 | 0.76 | 0.021 | 0.022 | 0.880 | 1.059 | 0.016 | 0.022 |
| MFRSR-UV _{USDA} | 332.16 | 3525 | 1.14 | 3.87 | 244.6 | 273.8 | 0.08 | 0.40 | 0.44 | 1.05 | -0.044 | 0.040 | 0.985 | 0.949 | -0.021 | 0.039 |
| | 355.00 ^{INTERP} | | | | | | 0.08 | 0.37 | 0.41 | 0.99 | -0.033 | 0.031 | 0.989 | 0.966 | -0.019 | 0.030 |
| | 368.13 | | | | | | 0.08 | 0.35 | 0.39 | 0.95 | -0.027 | 0.027 | 0.991 | 0.977 | -0.019 | 0.027 |
| R-Lidar(bscat) | 355.00 | 527 | 1.16 | 6.05 | 249.0 | 271.7 | 0.05 | 0.34 | 0.38 | 0.94 | -0.006 | 0.087 | 0.909 | 0.831 | 0.052 | 0.079 |
| R-Lidar (N ₂) | 355.00 | | | | | | 0.11 | 0.34 | 0.37 | 1.08 | -0.000 | 0.067 | 0.950 | 0.839 | 0.055 | 0.057 |

Results of Comparison

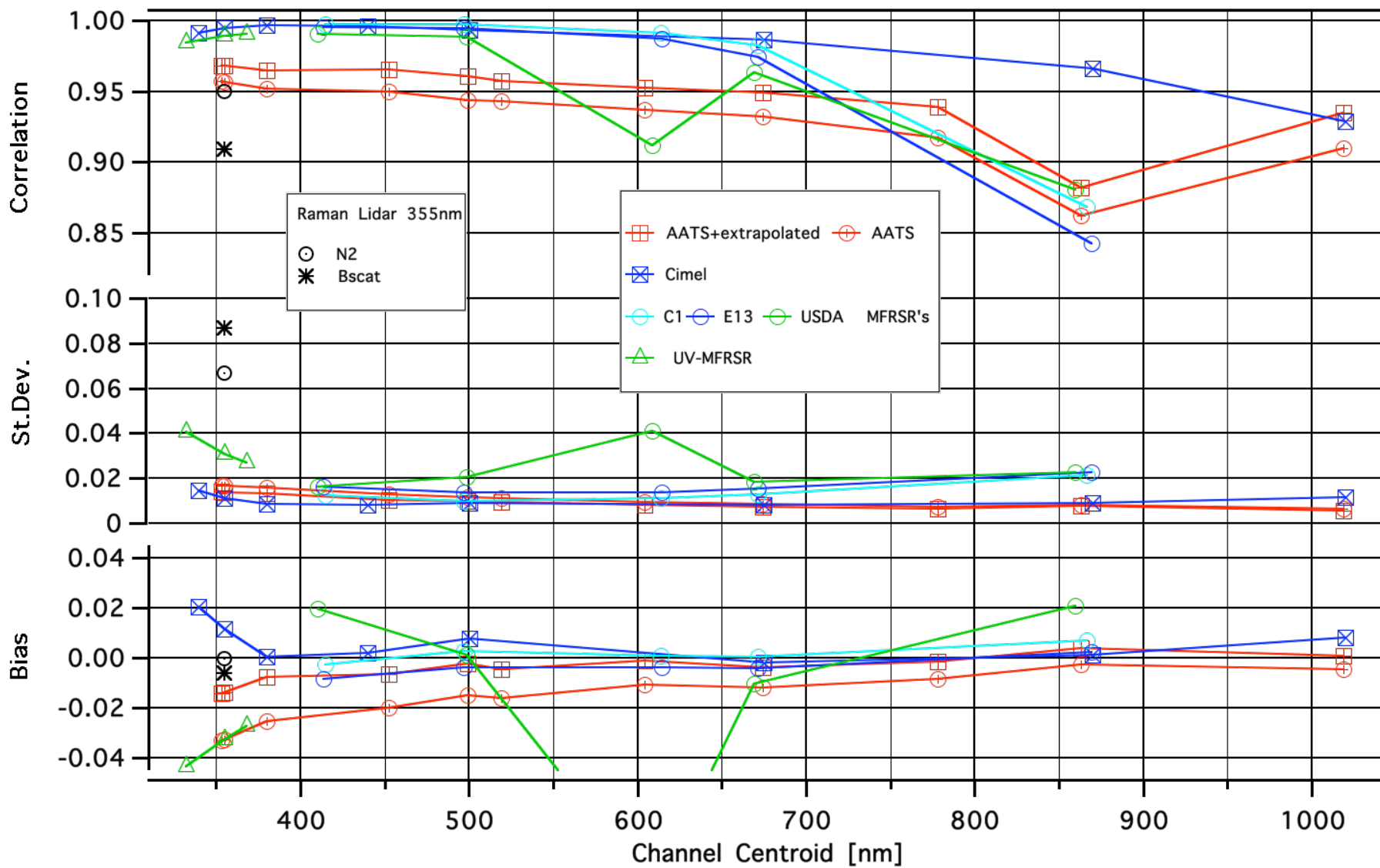
TABLE 3. AATS AOD's compared with RSS – cloud screening from MFRSR_{C1}

| Instrument | Channel centroids λ [nm] | Data Set Characteristics | | | | | | | | Comparison with RSS | | | | | | |
|--|-------------------------------------|--------------------------|------------------|------------------|------------------|------------------|------------------|---------|-------------|---------------------|---|----------------|-------------|----------|---------|--------------------|
| | | N_{pnts} | Airmass | | Time [doy] | | $y=\text{AOD}$ | | | | $y=\alpha x+\beta, x=\text{AOD}_{\text{RSS}}$ | | | | | |
| | | | A_{min} | A_{max} | d_{min} | d_{max} | y_{min} | μ_y | $2\sigma_y$ | y_{max} | μ_{y-x} | σ_{y-x} | $\rho(y,x)$ | α | β | rms_{fit} |
| AATS (airborne) | 353.49 | 55 | 1.22 | 3.16 | 256.7 | 265.6 | 0.11 | 0.21 | 0.10 | 0.31 | -0.033 | 0.017 | 0.957 | 0.835 | 0.007 | 0.014 |
| | 355.00 ^{INTERP} | | | | | | 0.11 | 0.21 | 0.10 | 0.31 | -0.033 | 0.017 | 0.957 | 0.836 | 0.007 | 0.014 |
| | 379.98 | | | | | | 0.10 | 0.19 | 0.09 | 0.29 | -0.026 | 0.016 | 0.952 | 0.854 | 0.007 | 0.014 |
| | 452.59 | | | | | | 0.08 | 0.15 | 0.07 | 0.23 | -0.020 | 0.013 | 0.950 | 0.846 | 0.007 | 0.011 |
| | 499.18 | | | | | | 0.07 | 0.13 | 0.06 | 0.20 | -0.015 | 0.012 | 0.944 | 0.844 | 0.009 | 0.010 |
| | 519.53 | | | | | | 0.07 | 0.13 | 0.06 | 0.19 | -0.016 | 0.011 | 0.943 | 0.832 | 0.008 | 0.010 |
| | 604.50 | | | | | | 0.05 | 0.10 | 0.05 | 0.15 | -0.011 | 0.009 | 0.937 | 0.819 | 0.010 | 0.008 |
| | 674.64 | | | | | | 0.05 | 0.08 | 0.04 | 0.12 | -0.012 | 0.008 | 0.932 | 0.785 | 0.009 | 0.007 |
| | 777.92 | | | | | | 0.03 | 0.07 | 0.03 | 0.10 | -0.008 | 0.007 | 0.917 | 0.797 | 0.007 | 0.006 |
| | 863.18 | | | | | | 0.03 | 0.06 | 0.03 | 0.09 | -0.003 | 0.008 | 0.862 | 0.812 | 0.010 | 0.008 |
| | 1018.49 | | | | | | 0.03 | 0.05 | 0.02 | 0.07 | -0.005 | 0.007 | 0.910 | 0.717 | 0.012 | 0.005 |
| AATS (airborne) with extrapolated ground layer AOD | 353.49 | 55 | 1.22 | 3.16 | 256.7 | 265.6 | 0.13 | 0.23 | 0.10 | 0.33 | -0.014 | 0.014 | 0.968 | 0.904 | 0.009 | 0.013 |
| | 355.00 ^{INTERP} | | | | | | 0.13 | 0.23 | 0.10 | 0.33 | -0.014 | 0.014 | 0.968 | 0.905 | 0.009 | 0.013 |
| | 379.98 | | | | | | 0.12 | 0.21 | 0.10 | 0.31 | -0.008 | 0.013 | 0.965 | 0.920 | 0.010 | 0.013 |
| | 452.59 | | | | | | 0.10 | 0.17 | 0.08 | 0.25 | -0.006 | 0.010 | 0.965 | 0.926 | 0.006 | 0.010 |
| | 499.18 | | | | | | 0.09 | 0.15 | 0.07 | 0.22 | -0.002 | 0.010 | 0.961 | 0.922 | 0.009 | 0.009 |
| | 519.53 | | | | | | 0.08 | 0.14 | 0.06 | 0.20 | -0.005 | 0.010 | 0.957 | 0.910 | 0.008 | 0.009 |
| | 604.50 | | | | | | 0.06 | 0.11 | 0.05 | 0.16 | -0.001 | 0.008 | 0.952 | 0.905 | 0.010 | 0.008 |
| | 674.64 | | | | | | 0.05 | 0.09 | 0.04 | 0.13 | -0.004 | 0.007 | 0.949 | 0.878 | 0.008 | 0.007 |
| | 777.92 | | | | | | 0.04 | 0.08 | 0.03 | 0.11 | -0.001 | 0.006 | 0.939 | 0.889 | 0.007 | 0.006 |
| | 863.18 | | | | | | 0.04 | 0.07 | 0.03 | 0.10 | 0.004 | 0.008 | 0.882 | 0.899 | 0.011 | 0.008 |
| | 1018.49 | | | | | | 0.03 | 0.06 | 0.03 | 0.08 | 0.001 | 0.005 | 0.935 | 0.821 | 0.011 | 0.005 |

Bias and standard deviation from Tables 2 and 3



Bias, standard deviation and correlation from Tables 2 and 3



Conclusions

Airborne data from AATS compare well with other instruments after AOD's were extrapolated to ground level using AATS derived extinction profiles.

For wavelengths larger than 380nm all instruments agree to within $\pm 0.01\text{OD}$ with the exception of 3 channels of MFRSR_{USDA}. The standard deviations are also small ($< 0.015\text{OD}$).

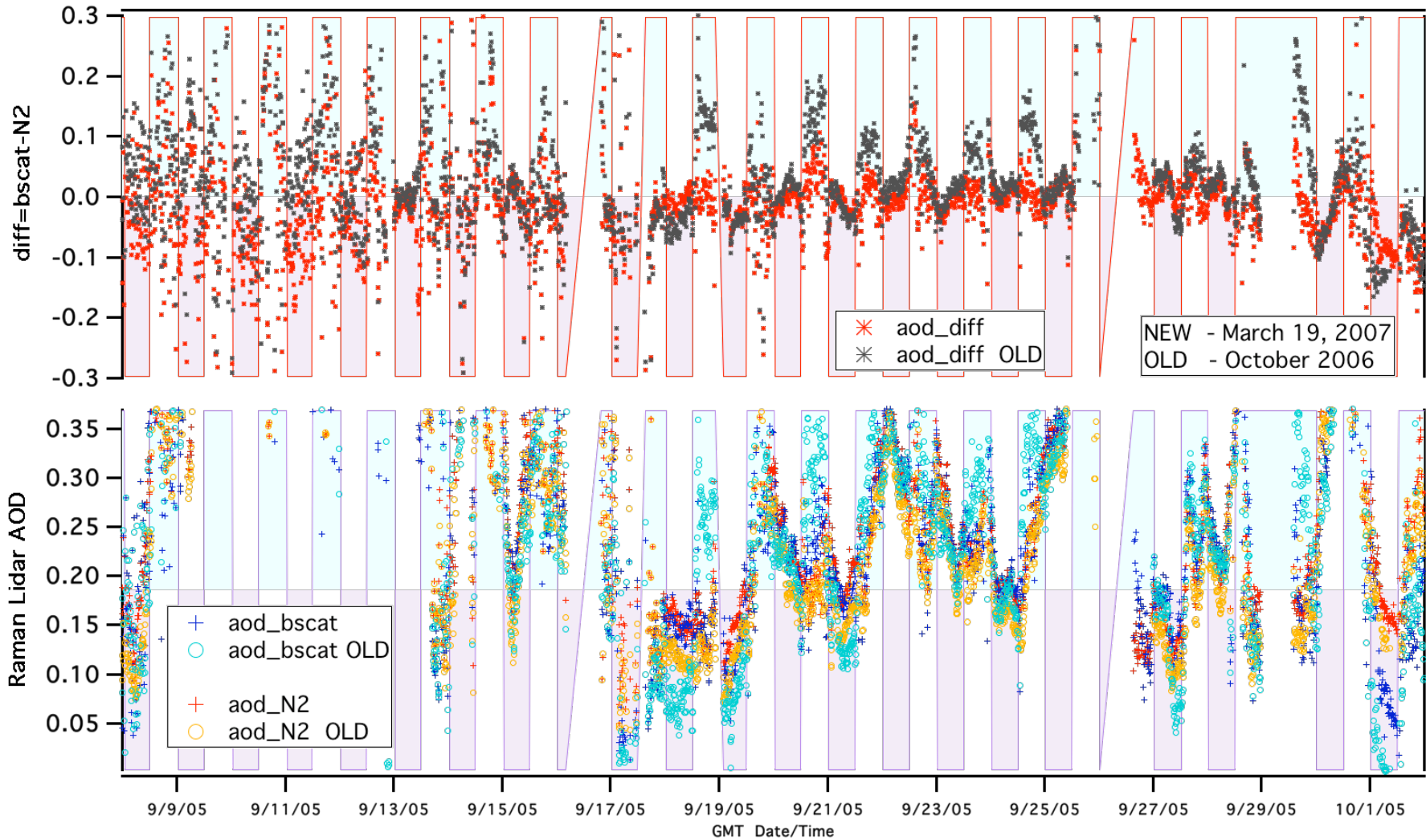
All three MFRSR's exhibit larger standard deviation at 870nm channel and the lower correlation than Cimel. The correlations are the lowest among all measurements.

In UV RSS extrapolated AOD's split the difference between Cimel and UV-MFRSR. The 332nm channel of UV-MFRSR reads 0.04OD too low and Cimel's 340nm channel reads 0.02OD too high. However Cimel 380nm channel produces one of the lowest biases $0.00025 \pm 0.0084\text{OD}$ closely followed by AATS 380nm channel with $-0.00077 \pm 0.013\text{OD}$ bias.

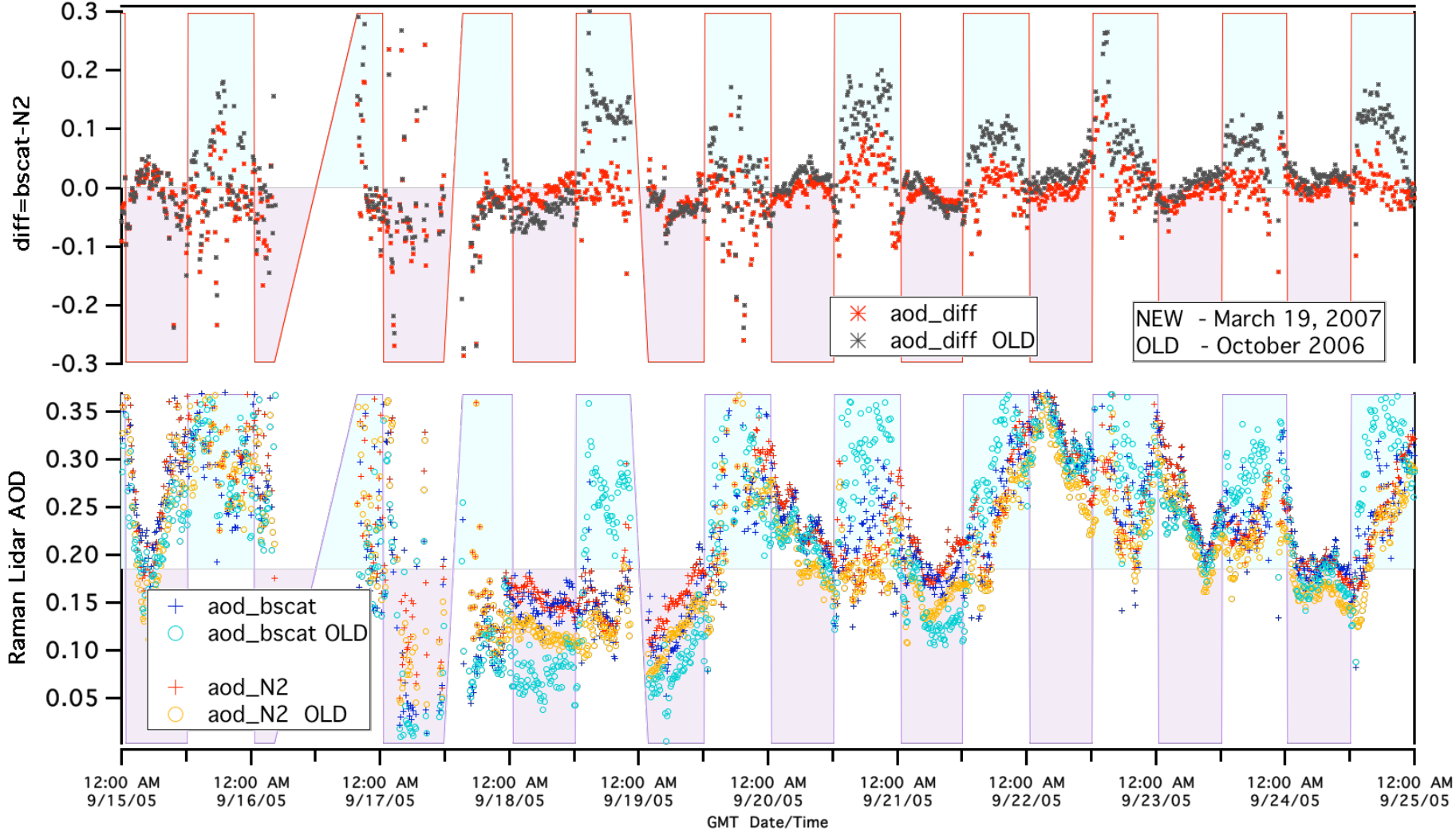
The two sets of Raman Lidar data produce surprisingly low bias -0.0005OD and -0.006OD for N_2 and backscatter derived AOD's, respectively. These biases are smaller than biases of interpolated at 355nm values from bracketing channels of Cimel, UV-MFRSR and AATS. But the Raman Lidar data exhibits the largest standard deviations: $\pm 0.066\text{OD}$ and $\pm 0.086\text{OD}$ for N_2 and backscatter, respectively.

Extra Slides

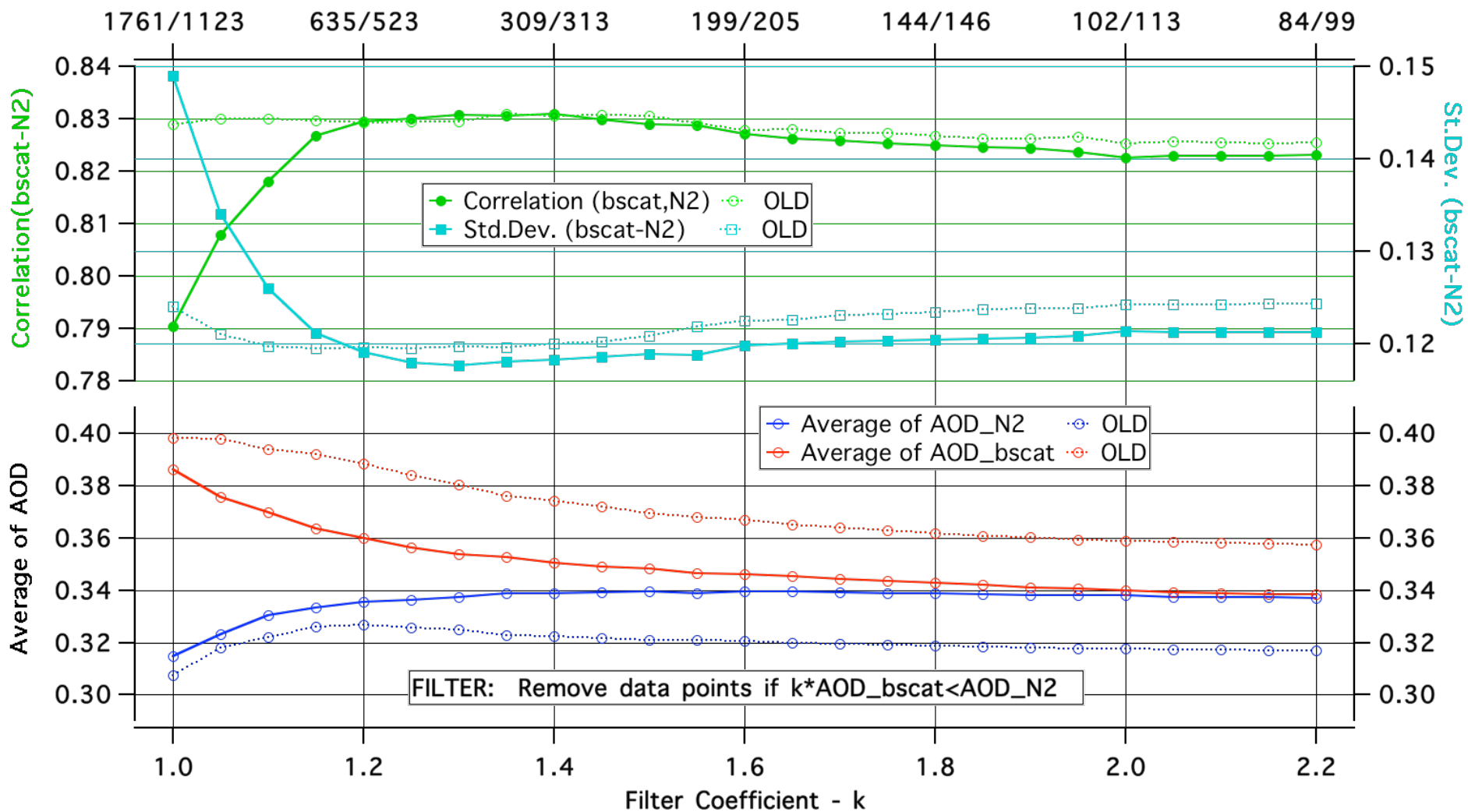
New (March 19, 2007) and Old (November 2006) RL Data Sets

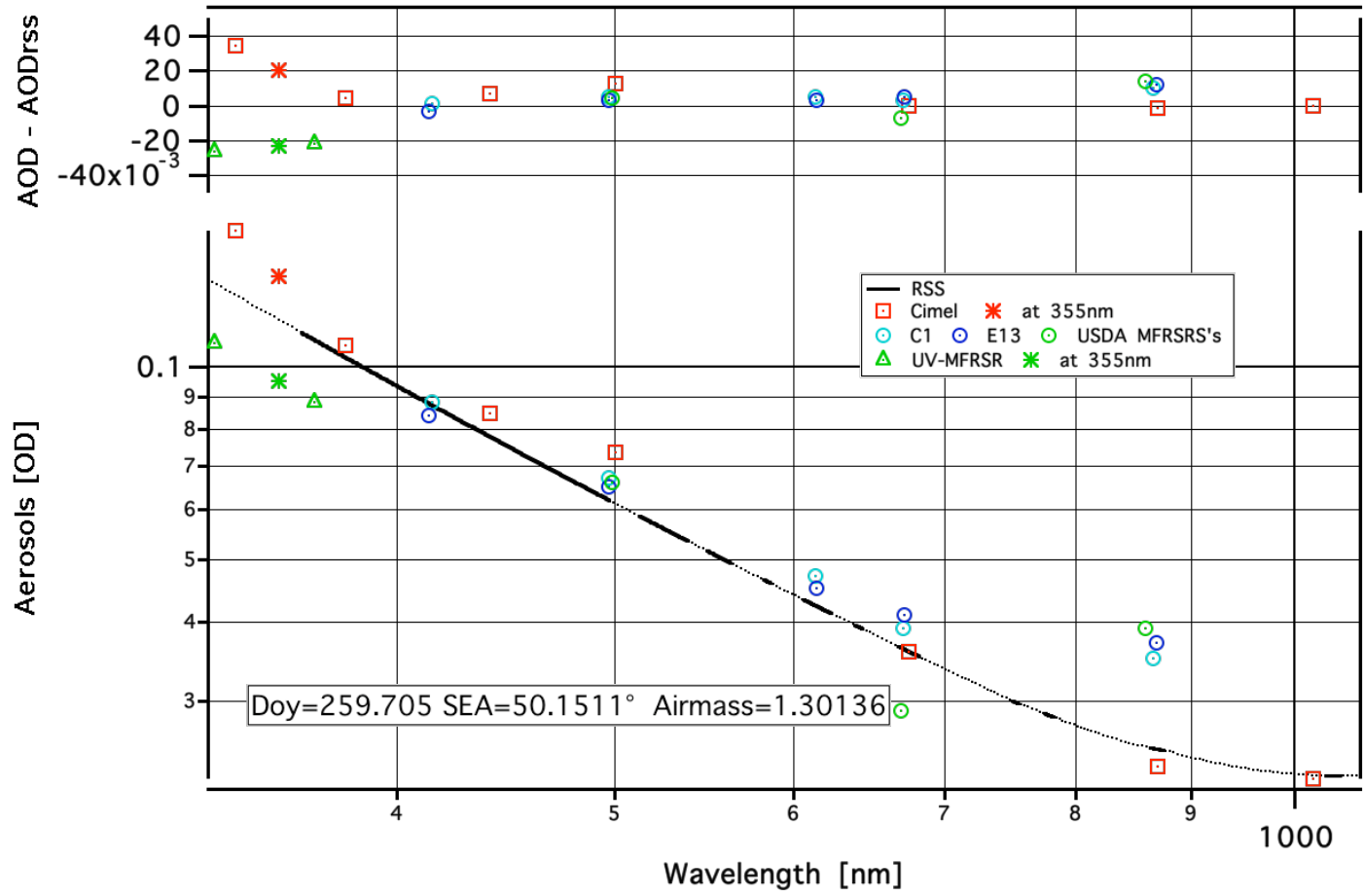


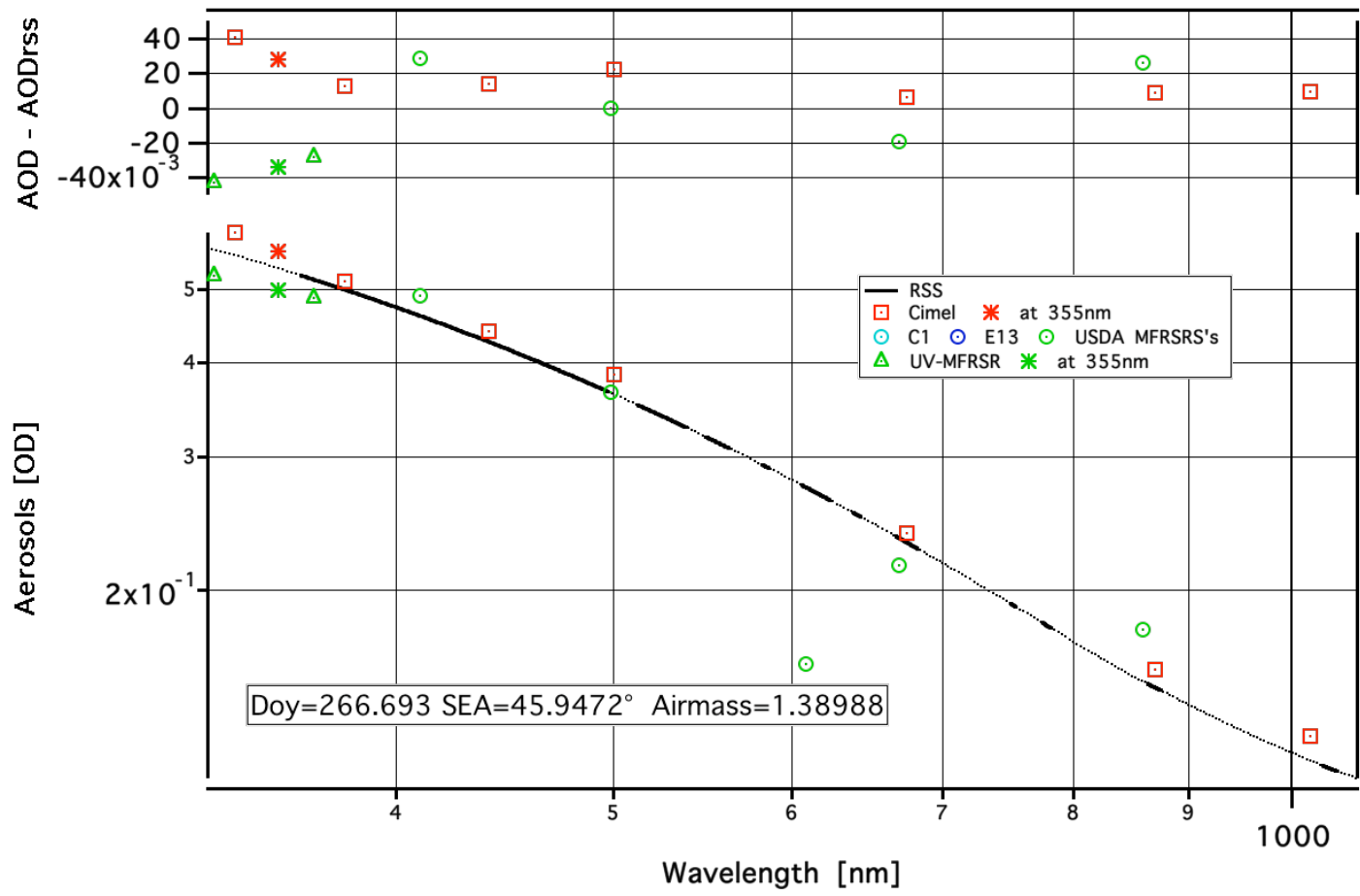
New (March 19, 2007) and Old (November 2006) RL Data Sets



Data points removed by filter out of Raman Lidar 2973 (2920 OLD) points







Channel 870nm water vapor contamination?

